Friction Stir Welding of Ultrafine Grained IF and Carbon Steels†

FUJII Hidetoshi*, UEJI Rintaro**, CUI Ring***,
NAKATA Kazuhiro**** and NOGI Kiyoshi ****

Abstract

The friction stir welding (FSW) of two kinds of ultrafine grained steel was performed. Ultrafine grained IF steel was produced by the accumulative roll bonding (ARB) process and the ultrafine grained low carbon steel (SM490) was produced by the Martensite process. The tensile strengths of the joints for all the materials are much higher than those of the TIG welds and increase with the increasing revolutionary pitch due to the decrease in grain growth. High strength joints are obtained for the ultrafine grained steel under the optimal welding and heat treatment conditions.

KEY WORDS: (Friction Stir Welding), (IF Steel), (Low Carbon Steel), (Accumulative Roll Bonding), (Martensite Method), (Ultrafine Grained Microstructure), (Tensile Strength), (Hardness)

1. Introduction

Significant attempts have recently been made to improve the mechanical properties of materials by controlling their microstructure. Grain refinement is one of the useful methods for enhancing mechanical properties[1,2]. According to the Hall-Petch relationship [3,4], the strength can be increased several times by producing ultrafine grains which are less than 1μm. However, the welding or joining of small parts is an essential processing step to make large or complex structures because it is difficult to directly manufacture a large or complex structure with ultrafine grains.

If fusion welding is applied to ultrafine grained materials, grain growth easily occurs and the strength decreases. On the other hand, friction stir welding (FSW) can inhibit the grain growth because a lower heat is input during the FSW [5-9]. Thus, FSW should be a better welding method for ultrafine grained metals than fusion welding.

FSW has been mainly used for aluminum alloys because high melting temperature materials, such as steel, are difficult to be FS-welded due to the absence of a proper tool. In this study, FSW was performed for ultrafine grained IF steel and carbon steel using a newly developed tool[6,7,10-13]. The ultrafine grains were made by the accumulative roll-bonding (ARB) processs[2,14] or by the new Martensite process[15,16].

2. Experimental

The materials used in this study were interstitial free steel (IF steel: 20ppmC), a plain carbon steel (SM490). The dimensions of the rectangular samples were 1.6mm thick, 300mm long and 30mm. These samples were butt-welded along the rolling direction (RD) using an FSW machine. The tool had a 12mm shoulder diameter and 4mm probe diameter. The probe length was 1.4mm. The tool was tilted by 3 degrees. The rotation speed and the traveling speed were 400rpm and 100-400mm/min for IF steel, 100mm/min and 250-600rpm for the plain carbon steel, respectively. Based on these conditions, the range of the revolutionary pitches was 0.25-1.0 mm/r for the IF steel, 0.17-0.40 mm/r for the plain carbon steel. Ar

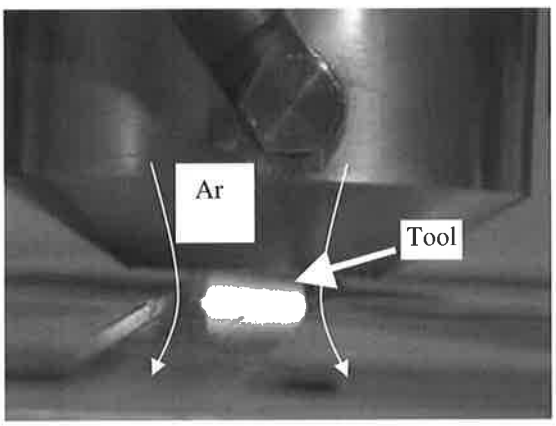

Fig.1 Appearance of FSW of steel.

† Received on May 12, 2006
* Associate Professor
** Research Associate, Kagawa University
*** Graduate Student
**** Professor
Transactions of JWRI is published by Joining and Welding Research Institute, Osaka University, Ibaraki, Osaka 567-0047, Japan

shielding gas was used during the friction stir welding of the steels, as shown in **Fig.1** The temperature of the bottom surface at the weld center of the sample was measured using thermocouple during the welding.

For the ARB process shown in **Fig.2**, two sheets were layered to make the degreased and brushed surface closely fixed to each other by clips. Roll bonding was conducted by a 50% reduction in one pass. In order to obtain a sufficient bonding strength, the samples were heated in a furnace at 773K for 10min before each pass. After the roll bonding, the samples were cooled immediately in water and then cut into two pieces. To produce the ultrafine grains, this procedure was repeated 5 times for the IF steel. High angle boundaries were introduced in these materials by this method. As a result, the strength of the IF steel increased to 775MPa. Some of the ARB samples were subsequently annealed at 600°C for 1.8ks.

The martensite process was applied to the commercial plain low carbon steel sheets (JIS-SM490, 0.14mass%C-0.64%Mn-0.002%N-0.01%Si-0.013%P-0.002%Nb-0.02 %Nb-Fe, 2.3mm thick, 30mm wide and 300mm long). This novel process allows an ultrafine grained microstructure to be obtained in plain carbon steel without severe plastic deformation (SPD) techniques such as ARB. The key to the martensite process is to use a martensite structure as the starting microstructure in the thermomechanial process, as shown in **Fig.3**. Only conventional cold-rolling to a strain of about 0.5 and post annealing at a warm temperature around 773K can produce the multiphased ultrafine microstructure which consists of 100-200nm ultrafine ferrite grains, uniformly precipitated carbides and tempered martensite blocks. It has been also clarified that multiphased ultrafine grained steels have a superior high strength with adequate ductility.

The as-received specimen has a ferrite + pearlite structure, so that, first of all, the as-received specimen

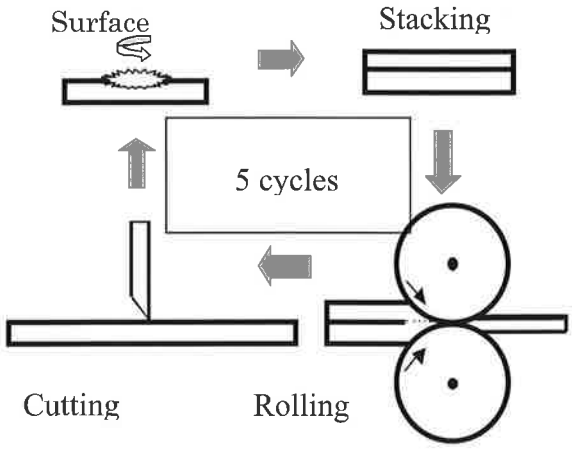

Fig.2 Schematic illustration showing the principle of accumulative roll-bonding.

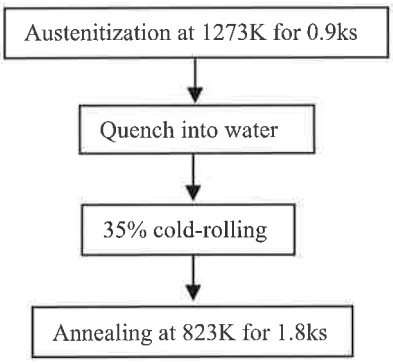

Fig.3 Martensite Process.

was austenitized at 1273K for 0.9ks followed by water-quenching to obtain a martensite microstructure. The as-quenched specimen was cold-rolled to a reduction in thickness of 35% and subsequently annealed at 823K for 1.8ks.

In order to evaluate the mechanical properties of the joints, the tensile strength and Vickers hardness were measured. The microstructural observations were performed by transmission electron microscopy (TEM) and an electron backscatter diffraction pattern (EBSP) analysis. Thin foils parallel to the transverse direction (TD) of the samples were prepared for TEM observation by twinjet electropolishing in a 90% CH_3OH + 10%$HClO_4$ solution for the steels. A Hitachi H-800 microscope was operated at 200kV. The EBSP measurements were carried out using a program developed by TSL (OIM-Analysis3.0x) in a Phillips XL30 SEM equipped with an FE-gun operated at 20kV. The planes parallel to the TD were cut from the weld and scanned by EBSD. A Vickers hardness test was conducted along the TD to evaluate the hardness profiles of the center at the thickness.

3. Results and Discussion

3.1 Ultrafine Grained IF Steel

3.1.1 Effect of Welding Conditions

Figure 4 shows an optical micrograph of the transverse section of the ARB processed steel joint. The welding center shows high degree of continuity and no defects. The temperatures of the bottom surfaces of the samples were around 650°C at the maximum during FSW, which is much lower than the α/γ transformation temperature (around 910°C).

Fig.4 Optical micrograph of transverse section of weld zone of ARB processed steel.

Figure 5 shows the tensile strength of the IF steel joints welded at different revolutionary pitches (welding speed / rotation speed). For the ultrafine grained IF steel, the tensile strengths of the joints increased with the increasing revolutionary pitch and all the samples were fractured in the stir zone. The strength of the ultrafine grained IF steel joints by FSW was much higher than that of the TIG joint (258MPa) though the strength decreased compared to that of the base material. On the other hand, for the normal grained IF steel, all the samples were fractured in the base material. For the normal grained IF steel, in order to measure the strengths of only the welded parts, tensile test specimens were made parallel to the welding direction. In this case, the strengths of the normal grained IF steel joints increased with the increasing revolutionary pitch.

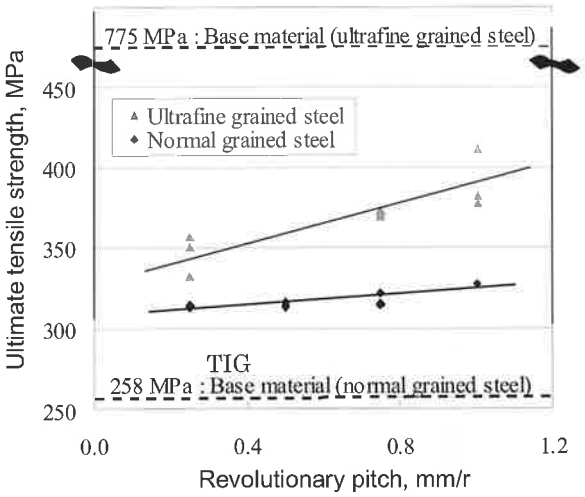

Fig.5 Tensile strength of IF steel joints welded at different revolutionary pitches.

3.1.2 Effect of Initial Grain Size

Figure 6 shows a color map indicating the crystallographic orientations of the as-received (a), the ARB processed (b) samples. (c) is an annealed sample of the ARB processed sample. These color maps were obtained by EBSD measurements and the horizontal and the vertical directions in this figure are parallel to the TD and nominal direction (ND), respectively. The colors determined in the stereographic triangle indicate the crystallographic orientation parallel to the RD. The black lines are high-angle boundaries with misorientations higher than 15°. The as-received sample (a) shows the equiaxed grains whose mean grain size is 24.2μm. The ARB processed samples shows a lamellar structure elongated parallel to the TD. The mean spacings of the high-angle boundaries along the ND and TD are 0.3μm and 1.6μm, respectively and the mean grain size is 0.7μm. During the annealing of the as-ARB samples, grain growth takes place and the shape of the grain becomes somewhat equiaxed but still keeps its elongated feature. The mean grain size of the annealed sample is 1.8μm.

The RD orientation color maps at the center of the thickness of the stir zone in the three FS welded samples are shown in **Fig.7**. The green color showing the [011]//RD orientation is dominant in both the as-received and the as-ARB processed samples, while the mixture of many colors are detected, indicating the existence of various orientations in the stir zone of the annealed samples. In all three samples, the color changes inside some grains surrounded by black lines, indicating the existence of subgrains and/or dislocations. The mean grain sizes surrounded by high-angle boundaries in the stir zone of the as-received, the ARB processed and the annealed samples are 5.3μm, 3.1μm, and 2.0μm, respectively.

Figure 8 shows the TEM bright field images of the stir zones in the as-received (a), the as-ARB processed (b) and the annealed (c) samples. The microstructures of all three samples consist of equiaxed grains including dislocations. The dislocation density seems to be higher than that in the stir zone in the FSW processed commercial purity aluminium reported in a previous study [5]. This is caused by the restricted recovery during the FSW process due to the lower maximum temperature (923K) reached by FSW, compared with the melting temperature of the steel (1811K). The mean grain size, observed in the TEM images of the as-received, the as-ARB processed and the annealed samples are 2.4μm, 1.1μm and 0.9μm, respectively. All these values are smaller than those obtained by the EBSD measurements.

These determinations of the smaller grain size by TEM are probably due to the existence of the low-angle grain boundaries in the stir zone for all the samples, although the difference in the observation (or measurement) direction between the TEM and EBSD is another possible reason. Anyhow, it can be clarified by both TEM observations and EBSD measurements that the hardness in the stir zone is higher with the decreasing (sub)grain sizes.

The hardness profiles along the TD of the samples after FSW are shown in **Fig.9**. The mean hardness of the base metals of the as-received, the ARB processed and the annealed samples are 91Hv, 222Hv, and 163Hv, respectively, indicating that the hardness increases with the decreasing mean grain size. The hardness of the as-received and the ARB processed samples are changed in the stir zone. The hardness of the stir zone in the as-received sample increases to 120Hv, whereas that in the as-ARB processed samples decreases to about 125Hv. The stir zone in the ARB processed sample is slightly harder than that in the as-received. On the other hand, concerning the annealed sample, the hardness of the stir zone is slightly decreased, however, it still maintains a high hardness around 150Hv. It should be noted that the stir zone in the annealed sample shows a higher hardness than those of the other two samples.

The grain size and hardness data are summarized in **Table 1**. The most important finding of the above experiments is that the annealed sample with the

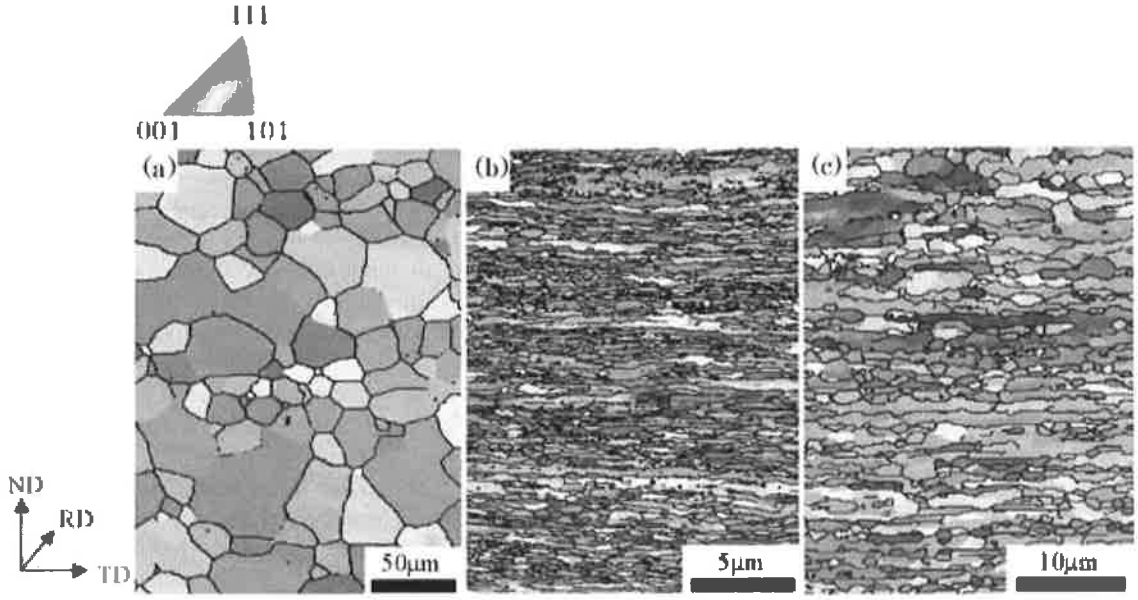

Fig.6 OIM of IF steel base material obtained by EBSP measurement.
(a) As received (b)ARB processed (c) Annealed steels.

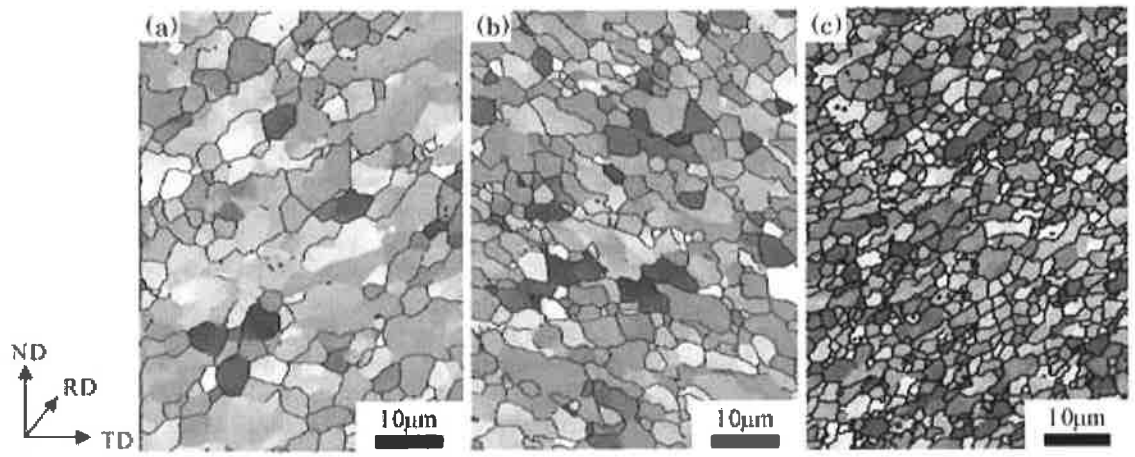

Fig. 7 OIM of stir zone obtained by EBSP measurement.
(a) As received (b)ARB processed (c) Annealed steels.

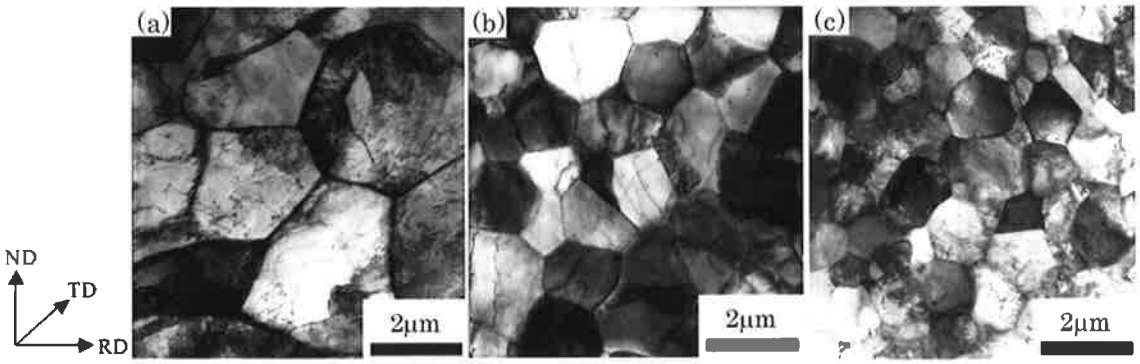

Fig.8 TEM bright field images of stir zone. (a) As received (b)ARB processed (c) Annealed steels.

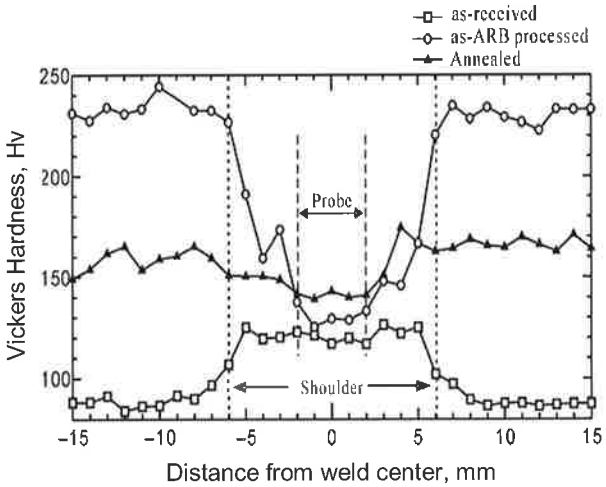

Fig. 9 Hardness profile of steel joints welded.

intermediate grain size (or intermediate hardness) in the base metal has the highest hardness in the stir zone after the FSW. It has been clarified that FSW gives rise to a large plastic flow in the stir zone, which causes the introduction of many dislocations and grain subdivision [17] by the dislocation boundaries to evolve fine grained microstructure. The dislocations and fine grains contribute to the strengthening of the stir zone. On the other hand, the heat generation by the plastic deformation provides the driving force of the recovery; the annihilation of the dislocation and the subgrain growth, resulting in decreasing the hardness. Generally, the generated heat is corresponding well to the plastic deformation energy which is the integration of the flow stress and strain. It is predictable that the flow stress of the as-ARB processed sample is the highest and the largest heat is then generated to enhance the recovery during the FSW process in this study. On the other hand, in the as-received sample with a lower flow stress, the heat generation is smaller and the stir zone is then strengthened. However, the hardness of the base metal is smallest of the three so that the hardness in the stir zone becomes smaller than those of the as-ARB and the annealed samples. Consequently, the intermediate hardness in the base metal is preferable for obtaining a high hardness in the stir zone, due to the balance between the strengthening by the plastic flow and the recovery. However, the work hardening behaviors should be different between the steels with conventional grain size and ultrafine gains [18], which makes it difficult to estimate the flow stress. In addition, although the geometric conditions are the same as shown in this study, the difference in the flow stress could cause the difference in the plastic flow behavior. Furthermore, the difference in the dislocation density between the deformed and the annealed states is another possible reason to inhibit the grain growth during FSW. These should be further studied to clarify the solid and logical relationships between the hardness of the stir zone and the base metal

3.2 Ultrafine grained carbon steel

Figure 10 shows the effect of the revolutionary pitch (heat input) on the hardness profile of the ultrafine grained carbon steel joint. The hardness of the stir zone decreases from the base material. When the heat input decreases (the revolutionary pitch increases), the volume of the softened region decreases. However, the hardness value of the minimum hardness region does not significantly change.

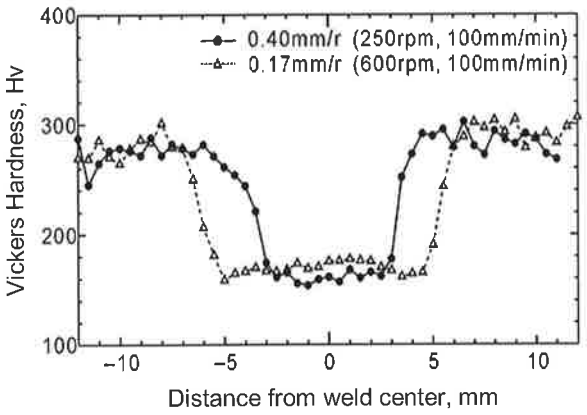

Fig.10 Effect of revolutionary pitch on hardness profile of ultrafine grained carbon steel joints.

Table 1 Mean grain size and hardness of base metal and stir zone of steels.

	Base metal		Stir zone		
	Grain size (EBSD), d_{Base} /μm	Hardness, H_{Base} / Hv	Grain size (EBSD), $d_{stir,EBSD}$ / μm	Grain size (TEM), $d_{stir,TEM}$/μm	Hardness, H_{stir} / Hv
As-received	24.2	91	5.3	2.4	120
As-ARB processed	0.7	222	3.1	1.1	125
Annealed	1.8	163	2.0	0.9	150

The base material consists of 100-200nm ferrite grains with uniformly precipitated carbide and tempered martensite blocks in the base metal. Consequently, the strength of the stir zone in the ultrafine grained joints decreased from the base material. However, note that more dislocations are also observed in the grains of the stir zone compared to that of the IF steel.

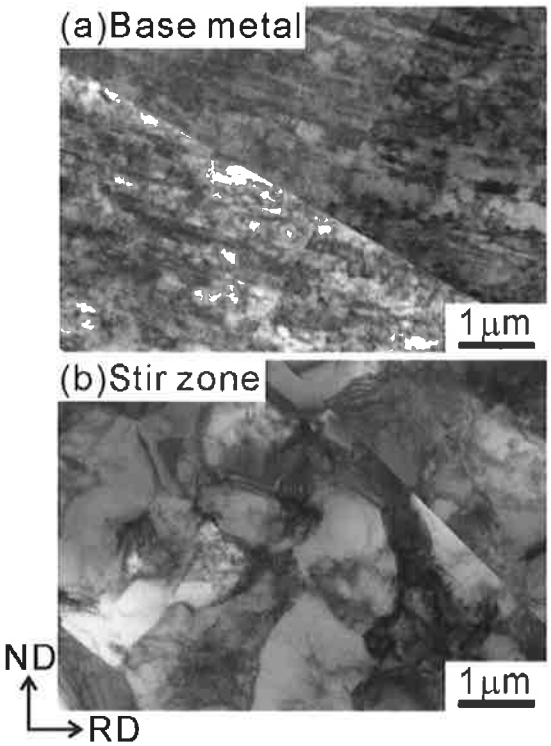

Fig.11 Bright field images of ultrafine grained carbon steel.

4. Summary

The hardness and microstructure of the FS welded IF and carbon steels with ultrafine grained microstructures fabricated by the ARB process or the Martensite method were investigated. Also, the effect of the initial grain size on the strength of the FSW joint was clarified. The important results of this study can be summarized as follows:

1. The tensile strengths of the IF steel and carbon steel joints welded by FSW significantly increases, compared to the TIG. The tensile strengths of all the joints increases with the increasing revolutionary pitch (with the decreasing heat input).
2. The grain size of the stir zone is significantly affected by the initial grain size of the samples. The mean grain size in the stir zone becomes smaller in order of the annealed sample, the ARB processed sample, and the as-received sample. The hardness of the stir zone increases with the decreasing mean grain size of the stir zone.
3. The steel with an intermediate grain size (1.8μm) is the most preferable to obtain the highest hardness in the stir zone with a small grain size.

Acknowledgment

The authors wish to acknowledge the financial support of the Toray Science Foundation, the Three Research Institute Project "Development Base of Joining Technology for New Metallic Glasses and Inorganic Materials, "Priority Assistance of the Formation of Worldwide Renowned Centers of Research - The 21st Century COE Program (Project: Center of Excellence for Advanced Structural and Functional Materials Design)" from the Ministry of Education, Sports, Culture, Science and Technology of Japan, and a Grant-in-Aid for Science Research from Scientific Research from Japan Society for Promotion of Science. The IF steel was provided by JFE Steel Co., Ltd. This support is gratefully appreciated by the authors.

References

1) T. C. Lowe and Y. T. Zhu, *Adv. Eng. Mat.* **5** (2003) 373.
2) N. Tsuji, Y. Saito, S. H. Lee and Y. Minamino, *Adv. Eng. Mat.*, **5** (2003) 338.
3) E.O..Hall, *Proc. Phys. Soc.*, **B64** (1951) 742.
4) N.J. Petch , *J. Iron Steel Inst.*, **174** (1953) 25.
5) Y. S. Sato, Y. Kurihara, S. H. C. Park, H. Kokawa and N. Tsuji,, *Scr. Mater.*, **50** (2004) 57.
6) H.Fujii, R.Ueji, Y.Takada, H.Kitahara, N.Tsuji, K.Nakata and K.Nogi, *Mater. Trans.*, **47** (2006) 239.
7) R.Ueji, H.Fujii, L.Cui, A.Nishioka, K.Kunishige and K.Nogi, *Mater. Sci. Eng. A*, **423** (2006) 324.
8) S. H. C. Park, Y. S. Sato, H. Kokawa, K. Okamoto, S. Hirano and M. Inagaki, *Scripta Mater.*, **49** (2003) 1175.
9) H. J. Liu, H. Fujii, M. Maeda and K. Nogi, *J. Mater. Sci. Lett.*, **22** (2003) 441.
10)Fujii, H, Takada, Y, Tsuji, N and Nogi, K, *Proc. 5th Int. FSW Symp.*, Metz, France,14-16 September, 2004, 04B-2.
11)H.Fujii, L.Cui, M.Maeda, K.Nogi, *Mater. Sci. Eng. A*, **419** (2006) 25.
12)H.Fujii, L.Cui, N.Tsuji, M.Maeda, K.Nakata and K.Nogi, *Mater. Sci. Eng. A*, **429** (2006) 50.
13)T.Ishikawa, H.Fujii, K.Genchi, L.Cui, S.Matsuoka and K.Nogi, *Q. J. Jpn Weld. Soc.*, **24** (2006) 174.
14) Saito, Y, Tsuji, N, Utsunomiya, H, Sakai, T and RG.Hong, *Scripta Mater.*, **39** (1998) 1221.
15) Tsuji, N, Ueji, R, Minamino, Y, Saito, Y, *Scripta Mater.*, **46** (2002) 305.
16) Ueji, R, Tsuji, N, Minamino, Y, Koizumi, Y, *Acta Mater.*, **50** (2002) 4177.
17)N.Hansen, X.Huang and D. A. Hughes, *Mater. Sci. Eng. A*, **317** (2001) 3.
18)N. Tsuji, Y. Ito, Y. Saito and Y. Minamino, *Scripta Mater.*, **47** (2002) 893.